



10/045,534, 116142-00230

PATENT
116142-00230

5

IN THE UNITED STATES PATENT AND TRADEMARK OFFICE

Applicants : Aprile L. Pilon
Serial No. : 10/045,534
Filed : October 24, 2001
For : METHODS AND COMPOSITIONS FOR THE TREATMENT
OF FIBROTIC CONDITIONS & IMPAIRED LUNG FUNCTION
& TO ENHANCE LYMPHOCYTE PRODUCTION
Group Art Unit : 1614
Examiner : Unassigned

919 Third Avenue
New York, New York 10022

I hereby certify that this correspondence
is being deposited with the United States
Postal Service as first class mail in an
envelope addressed to:
Assistant Commissioner for Patents,
Washington, D.C. 20231, on May 13, 2002

Robert E. Alderson, Jr. Reg. No. 44,500
Name of Applicant, Assignee or Registered
Representative

Robert E. Alderson, Jr.
Signature

May 13, 2002
Date of Signature

AMENDMENT AND RESPONSE TO NOTICE TO FILE MISSING PARTS

Assistant Commissioner for Patents
Washington, D.C. 20231

Sir:

This Amendment is submitted in response to the March 13, 2002 Notice to File Missing Parts of Nonprovisional Application issued by the United States Patent and Trademark Office in connection with the above-identified patent application.

In the specification:

Please delete the section entitled “Brief Description of the Drawings” on pages 17-20 of the specification. Below is a replacement “Brief Description of the Drawings” section to be inserted into the specification at pages 17-20 in place of the deleted section. A marked-up version of the “Brief Description of the Drawings” explicitly showing all amendments made herein is separately submitted herewith as **Exhibit A**.

–BRIEF DESCRIPTION OF THE DRAWINGS

The invention will now be described in more detail, with reference to the accompanying drawings, in which:

Figure 1 shows the standard curve obtained using the uteroglobin (UG) immunoassay described below.

Figure 2 shows the bicarbonate excess (BE) exhibited in pre-term lambs upon intratracheal administration of recombinant human uteroglobin.

Figure 3 shows the decrease in CO₂ exhibited in pre-term lambs upon intratracheal administration of recombinant human uteroglobin.

Figure 4 shows the increase in blood pH exhibited in pre-term lambs upon intratracheal administration of recombinant human uteroglobin.

Figure 5 shows the increase in paO₂/FiO₂ exhibited in pre-term lambs upon intratracheal administration of recombinant human uteroglobin.

Figure 6A shows the concentration of recombinant human uteroglobin (CC10) in serum as a function of time after intratracheal administration of recombinant human uteroglobin to newborn piglets.

Figure 6B shows the total protein concentration in BAL fluids obtained from piglets in each of the eight treatment groups.

Figure 7 shows the pressure-volume relationship observed upon administration of recombinant human uteroglobin to newborn piglets.

Figure 8 shows the mean pressure-volume relationship observed upon administration of

recombinant human uteroglobin to newborn piglets ventilated with 100% oxygen.

Figure 9 shows the mean pressure-volume relationships observed for all animals upon administration of recombinant human uteroglobin to newborn piglets ventilated with room air and 100% oxygen.

Figure 10A shows the mean pressure-volume curve among four treatment groups of newborn piglets administered recombinant human uteroglobin.

Figure 10B shows the mean pressure-volume curve among five treatment groups of newborn piglets administered recombinant human uteroglobin.

Figure 10C shows changes in PMN and lymphocyte cell counts over a 28-day period.

Figure 11 shows radioactive counts as a function of time for each group of Wistar rats administered recombinant human uteroglobin via intravenous administration.

Figure 12 shows radioactive counts as a function of time for each group of Wistar rats administered recombinant human uteroglobin via intranasal administration.

Figure 13 shows radioactive counts as a function of time for each group of Wistar rats administered recombinant human uteroglobin via stomach gavage.

Figure 14 shows the concentration of recombinant human uteroglobin as a function of time for each group of Wistar rats administered recombinant human uteroglobin via intravenous administration.

Figure 15 shows the concentration of recombinant human uteroglobin as a function of time for each group of Wistar rats administered recombinant human uteroglobin via intranasal administration.

Figure 16 shows the concentration of recombinant human uteroglobin as a function of time for each group of Wistar rats administered recombinant human uteroglobin via stomach gavage.

Figures 17A-17B are schematic representations of two ELISA-based assay formats for the uteroglobin-fibronectin binding interaction. Format A, shown in Figure 17A represents an assay based on immunodetection, wherein CC10 is uteroglobin and HRP is horse radish peroxidase. Format B, shown in Figure 17B represents a competitive binding assay format in which CC10 is uteroglobin, HRP is horse radish peroxidase, and rhFn is recombinant human

fibronectin, and the free uteroglobin in the same competes with the HRP-labeled uteroglobin for binding sites on recombinant human fibronectin.

Figure 18 shows a map of the human fibronectin protomer.

Figure 19 shows the results obtained from binding assays between uteroglobin (CC10) and intact and fragmented fibronectin using format A, wherein hFn is human fibronectin and SuperFn is superfibronectin.

Figures 20A-20B show the dose response curves for uteroglobin binding to fibronectin and its fragments using format A, wherein rhUG is recombinant human uteroglobin, hFn is human fibronectin, and Fn is fibronectin.

Figure 21 shows the mean change in airway resistance in perfused rat lung.

Figure 22 shows the mean concentration of TNF-alpha in BAL fluid from perfused rat lung.

Figure 23 shows a flow diagram of the maturation of hemopoietic stem cells.

Figure 24 shows ATPase activity in CD71-positive cells from rats treated with recombinant human uteroglobin.

Figure 25 shows ATPase activity in CD11b-positive cells from rats treated with recombinant human uteroglobin.

Figure 26 shows an *in vitro* wound healing assay with recombinant human uteroglobin.

Figures 27A and 27B show the inhibition of endothelial cell migration by recombinant human uteroglobin.

Figure 28 shows an extracellular matrix invasion assay with endothelial cells and recombinant human uteroglobin.

Figure 29A shows the endothelial cell growth curve with and without recombinant human uteroglobin.

Figure 29B shows the dose dependent response of endothelial cell VEGF stimulated proliferation assay.

Figure 30 shows a Western blot of proteins from three cell lines (Hfl-1, A59 and Hec-1A) probed with and recognized by anti-fibronectin monoclonal antibody. Lane 1 - Rainbow marker; Lane 2 - Hfl extract; Lane 5 - A549 extract; Lane 9 - Hec-1A extract.

Figure 31 shows colony counts of A549 soft agar assay, plate 2: 25 days. First row: control, second row: 0.2 μ M rhUG treated cells. No. of living cells or very small colonies (No. of well shaped colonies) in each well:

Row 1: 255 (109)	240(98)	293(120)
Row 2: 57(25)	89(44)	97(52)

Figure 32 shows a silver-stained SDS-Page gel indicating UG affinity purified bands that cross react with specific antibodies. Lane 1 - Rainbow marker; Lane 2 - membrane protein extract from Hec-1A, eluted from UG affinity column. Arrows indicate the protein bands that were recognized by anti-CD 148 antisera.

Figure 33 shows a competition curve for binding of rhCC10 to fibronectin.

Figure 34 shows binding of rhCC10 to fibronectin.--

REMARKS

In response to the Notice to File Missing Parts mailed December 10, 2001, Applicants submit herewith their signed Declaration and Power of Attorney (**Exhibit B**).

Also in response to the Notice to File Missing Parts, Applicants have amended the application to delete excess text from the drawings and to incorporate that text into the "Brief Description of the Figures". Accordingly, Applicants have included a replacement "Brief Description of the Figures" section (above). Applicants are also submitting a replacement set of drawings (**Exhibit C**, 28 sheets) and a marked-up set of Figures 30, 31 and 32 (pages 24, 25 and 26) showing changes in red ink (**Exhibit D**, 3 sheets).

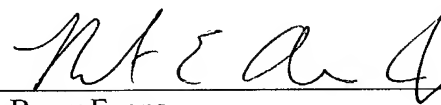
PATENT
116142-00230

Enclosed please find our Check No. 5573 in the amount of \$65.00 in payment of the fee for late filing of the declaration. In the event that any additional fees are due, please charge Deposit Account No. 50-0540.

Respectfully submitted,

KRAMER LEVIN NAFTALIS & FRANKEL LLP
Attorneys for Applicants

By: _____



Barry Evans
Reg. No. 22,802
(212) 715-7609
Robert E. Alderson, Jr.
Reg. No. 44,500
(212) 715-7697

**EXHIBIT A****Marked-up Version of "Brief Description of the Drawings"****--BRIEF DESCRIPTION OF THE DRAWINGS**

The invention will now be described in more detail, with reference to the accompanying drawings, in which:

Figure 1 shows the standard curve obtained using the uteroglobin (UG) immunoassay described below.

Figure 2 shows the bicarbonate excess (BE) exhibited in pre-term lambs upon intratracheal administration of recombinant human uteroglobin.

Figure 3 shows the decrease in CO₂ exhibited in pre-term lambs upon intratracheal administration of recombinant human uteroglobin.

Figure 4 shows the increase in blood pH exhibited in pre-term lambs upon intratracheal administration of recombinant human uteroglobin.

Figure 5 shows the increase in paO₂/FiO₂ exhibited in pre-term lambs upon intratracheal administration of recombinant human uteroglobin.

Figure 6A shows the concentration of recombinant human uteroglobin (CC10) in serum as a function of time after intratracheal administration of recombinant human uteroglobin to newborn piglets.

Figure 6B shows the total protein concentration in BAL fluids obtained from piglets in each of the eight treatment groups.

Figure 7 shows the pressure-volume relationship observed upon administration of recombinant human uteroglobin to newborn piglets.

Figure 8 shows the mean pressure-volume relationship observed upon administration of recombinant human uteroglobin to newborn piglets ventilated with 100% oxygen.

Figure 9 shows the mean pressure-volume relationships observed for all animals upon administration of recombinant human uteroglobin to newborn piglets ventilated with room air and 100% oxygen.

Figure 10A shows the mean pressure-volume curve among four treatment groups of newborn piglets administered recombinant human uteroglobin.

Figure 10B shows the mean pressure-volume curve among five treatment groups of

newborn piglets administered recombinant human uteroglobin.

Figure 10C shows changes in PMN and lymphocyte cell counts over a 28-day period.

Figure 11 shows radioactive counts as a function of time for each group of Wistar rats administered recombinant human uteroglobin via intravenous administration.

Figure 12 shows radioactive counts as a function of time for each group of Wistar rats administered recombinant human uteroglobin via intranasal administration.

Figure 13 shows radioactive counts as a function of time for each group of Wistar rats administered recombinant human uteroglobin via stomach gavage.

Figure 14 shows the concentration of recombinant human uteroglobin as a function of time for each group of Wistar rats administered recombinant human uteroglobin via intravenous administration.

Figure 15 shows the concentration of recombinant human uteroglobin as a function of time for each group of Wistar rats administered recombinant human uteroglobin via intranasal administration.

Figure 16 shows the concentration of recombinant human uteroglobin as a function of time for each group of Wistar rats administered recombinant human uteroglobin via stomach gavage.

Figures 17A-17B are schematic representations of two ELISA-based assay formats for the uteroglobin-fibronectin binding interaction. Format A, shown in Figure 17A represents an assay based on immunodetection, wherein CC10 is uteroglobin and HRP is horse radish peroxidase. Format B, shown in Figure 17B represents a competitive binding assay format in which CC10 is uteroglobin, HRP is horse radish peroxidase, and rhFn is recombinant human fibronectin, and the free uteroglobin in the same competes with the HRP-labeled uteroglobin for binding sites on recombinant human fibronectin.

Figure 18 shows a map of the human fibronectin protomer.

Figure 19 shows the results obtained from binding assays between uteroglobin (CC10) and intact and fragmented fibronectin using format A, wherein hFn is human fibronectin and SuperFn is superfibronectin.

Figures 20A-20B show the dose response curves for uteroglobin binding to fibronectin and its fragments using format A, wherein rhUG is recombinant human uteroglobin, hFn is human fibronectin, and Fn is fibronectin.

Figure 21 shows the mean change in airway resistance in perfused rat lung.

Figure 22 shows the mean concentration of TNF-alpha in BAL fluid from perfused rat lung.

Figure 23 shows a flow diagram of the maturation of hemopoietic stem cells.

Figure 24 shows ATPase activity in CD71-positive cells from rats treated with recombinant human uteroglobin.

Figure 25 shows ATPase activity in CD11b-positive cells from rats treated with recombinant human uteroglobin.

Figure 26 shows an *in vitro* wound healing assay with recombinant human uteroglobin.

Figures 27A and 27B show the inhibition of endothelial cell migration by recombinant human uteroglobin.

Figure 28 shows an extracellular matrix invasion assay with endothelial cells and recombinant human uteroglobin.

Figure 29A shows the endothelial cell growth curve with and without recombinant human uteroglobin.

Figure 29B shows the dose dependent response of endothelial cell VEGF stimulated proliferation assay.

Figure 30 shows a Western blot of proteins from three cell lines (Hfl-1, A59 and Hec-1A) probed with and recognized by anti-fibronectin monoclonal antibody. Lane 1 - Rainbow marker; Lane 2 - Hfl extract; Lane 5 - A549 extract; Lane 9 - Hec-1A extract.

Figure 31 shows colony counts of A549 soft agar assay, plate 2: 25 days. First row: control, second row: 0.2 μ M rhUG treated cells. No. of living cells or very small colonies (No. of well shaped colonies) in each well:

Row 1: <u>255 (109)</u>	<u>240(98)</u>	<u>293(120)</u>
Row 2: <u>57(25)</u>	<u>89(44)</u>	<u>97(52)</u>

Figure 32 shows a silver-stained SDS-Page gel indicating UG affinity purified bands that cross react with specific antibodies. Lane 1 - Rainbow marker; Lane 2 - membrane protein extract from Hec-1A, eluted from UG affinity column. Arrows indicate the protein bands that were recognized by anti-CD 148 antisera.

Figure 33 shows a competition curve for binding of rhCC10 to fibronectin.

Figure 34 shows binding of rhCC10 to fibronectin.--